Simulations and Experiments Toward Enabling Direct Power Extraction Application

NETL – Research and Innovation Center

Presented by Rigel Woodside --- Rigel.Woodside@netl.doe.gov

Co-Authors: Nate Weiland, Peter Hsieh, Clint Bedick, E. David Huckaby, Jasper Kwong, Lee Aspitarte, Michael Bowen, Jason Mazzoccoli, Chuck White, Hyoungkeun Kim, David Cann

2018 NETL Crosscutting Research Conference, 4/12/2018

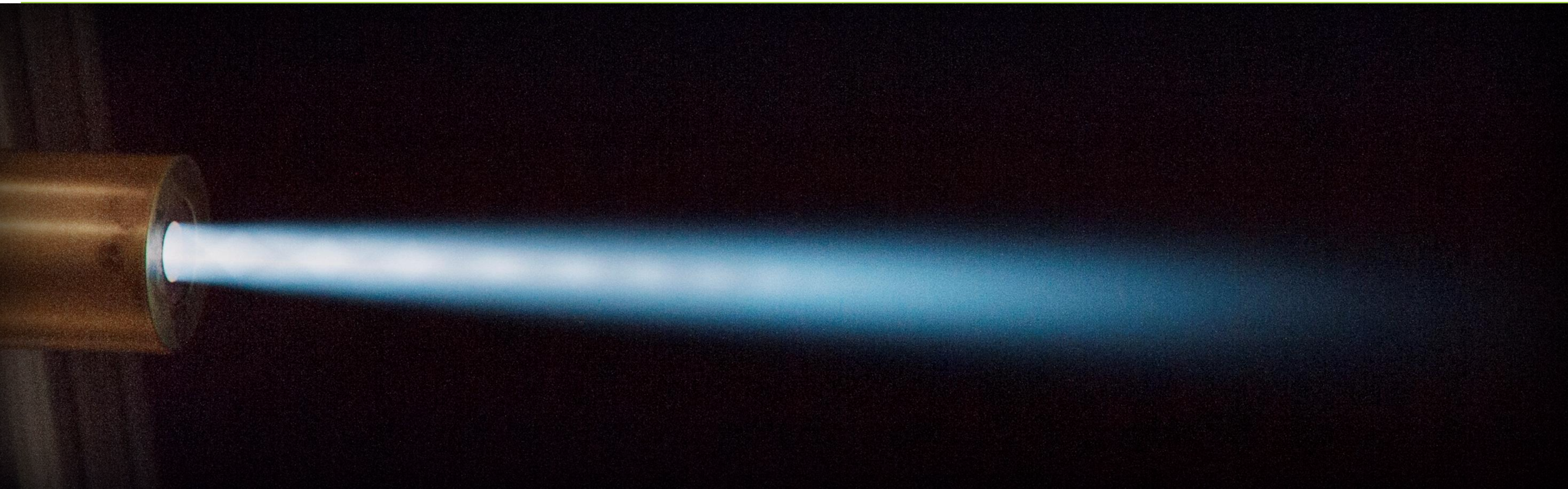

Presentation Outline

NETL RIC Current Activity Summary for Systems Engineering & Analysis, Energy Conversion Engineering, Materials Science & Engineering

- **Introduction**
- **Combined Cycle DPE Systems - Scoping & Analysis**
- **Oxy-Fuel Combustion Plasma Conductivity**
- **Multi-phase HVOF Simulation**
- **MHD Electrodes & Testing**
- **Photoionization Simulation & Experiment**
- **Conclusion**

Introduction

Goal: Determine if MHD Power Generation is a technically feasible option for future coal-power generation and develop a technology road map to get there

Objective: Produce engineering data sets, simulation tools and materials and perform a robust performance assessment for the technology

Approach: Apply systems level modeling to screen the various technology options; Develop, utilize, and validate simulations to predict the performance of components in those systems

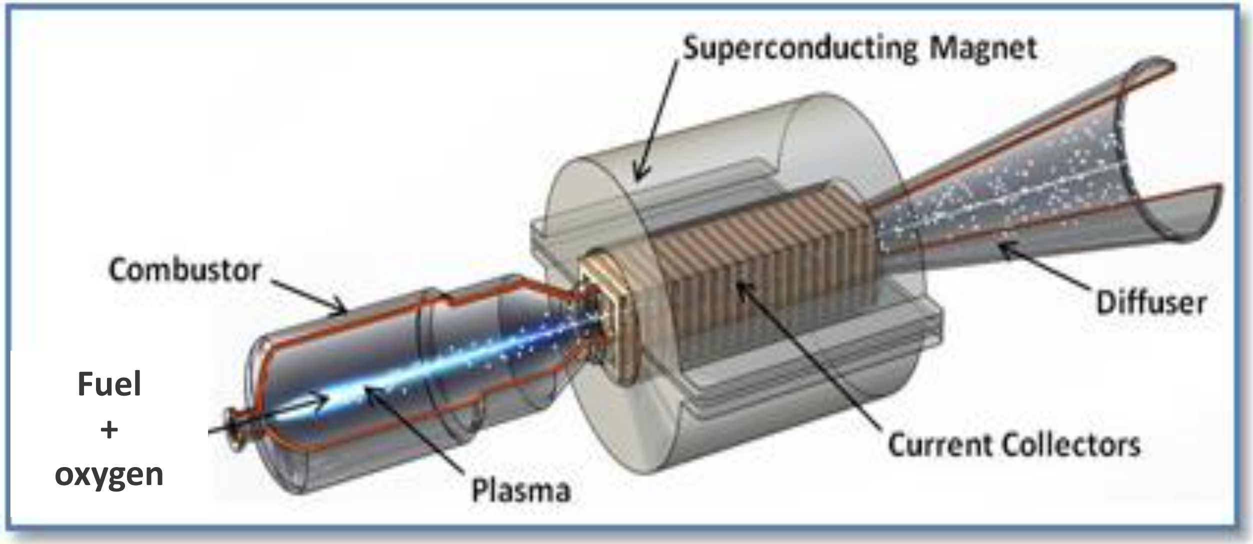

$$P \propto \sigma B^2 u^2$$

P is the power density
B is applied magnetic field
σ is gas-plasma conductivity
u is gas-plasma velocity

DPE Systems Scoping Study

Objectives and Methodology

- **Objective: Identify DPE systems that meet USDOE cost of electricity (COE) goals, as well as those that provide other benefits (modularity, low water etc.)**
  - Present study focused on DPE systems with carbon capture
  - Expanded FY18 study to add non-capture DPE systems
- **Approach: Use simplified analyses to direct NETL's future detailed systems analyses towards promising systems that incorporate DPE/magnetohydrodynamics (MHD) in new and potentially beneficial ways**
  - Investigated both open and closed cycle MHD, with coal and natural gas fuels
  - Analyzed with assistance from DPE experts from NETL and universities
  - Qualitative analysis phase included:
    - Evaluations of 15 systems against 14 qualitative rating criteria
    - Down-selection of 7 promising configurations for semi-quantitative analysis
  - Semi-quantitative analysis phase included:
    - Development of "Black box" component and system modeling approach using Aspen Plus
    - Selection of several NETL non-MHD reference cases for comparison basis
    - Templates for performance reporting, mass/energy balances, and stream table generation
    - Approximate MHD channel sizing and component costing for open cycle MHD options

DPE System Concept
Baseline DPE with Oxy-combustion, DPE-AUSC
CO_2 Recycle DPE System*
Natural Gas DPE System w/Recycle
High Potassium Biomass Seeding
Top Gasification DPE Steam Combined Cycle
DPE Topping w/ Coal Gasif. and Fuel Preheater
Tail Gasification DPE/GT/ST
OC Disc DPE/Steam Cycle w/ CO2 Recovery
Photoionization DPE
Seedless DPE Power Generation*†
Pulse Detonation DPE*†
Noble Gas Closed Cycle DPE
Triple cycle: OC DPE/CC DPE/AUSC Steam
Triple cycle: SOFC/DPE/Steam
Closed Cycle DPE/Steam Plant
DPE and sCO2 Bottoming Cycle

* External collaborator † Deferred to FY18

Scoping Study Efficiency Results

NATIONAL ENERGY TECHNOLOGY LABORATORY

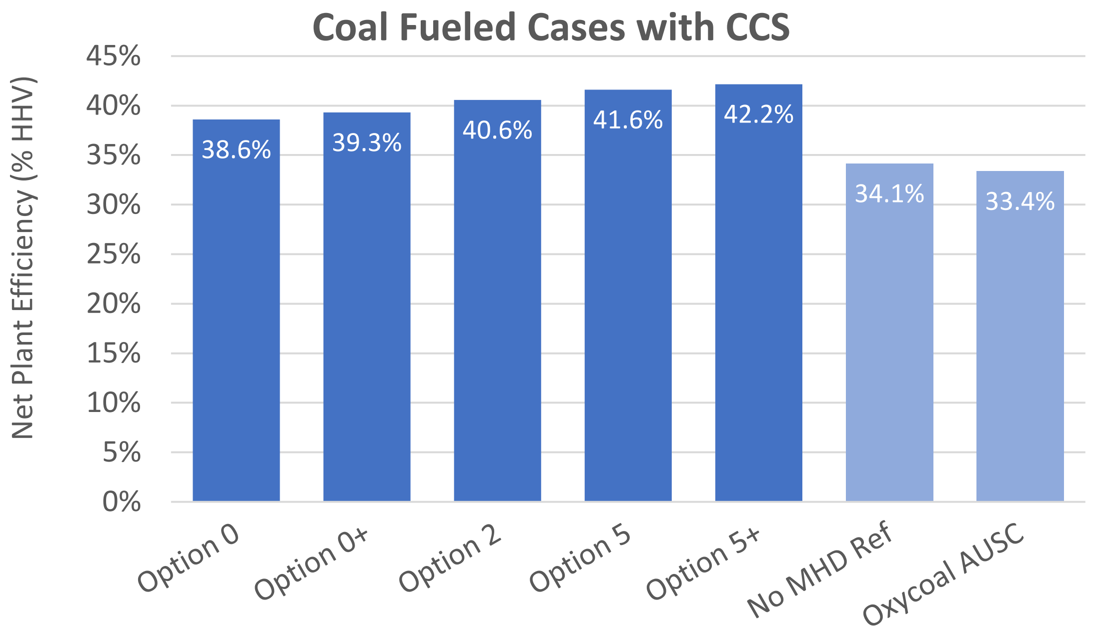

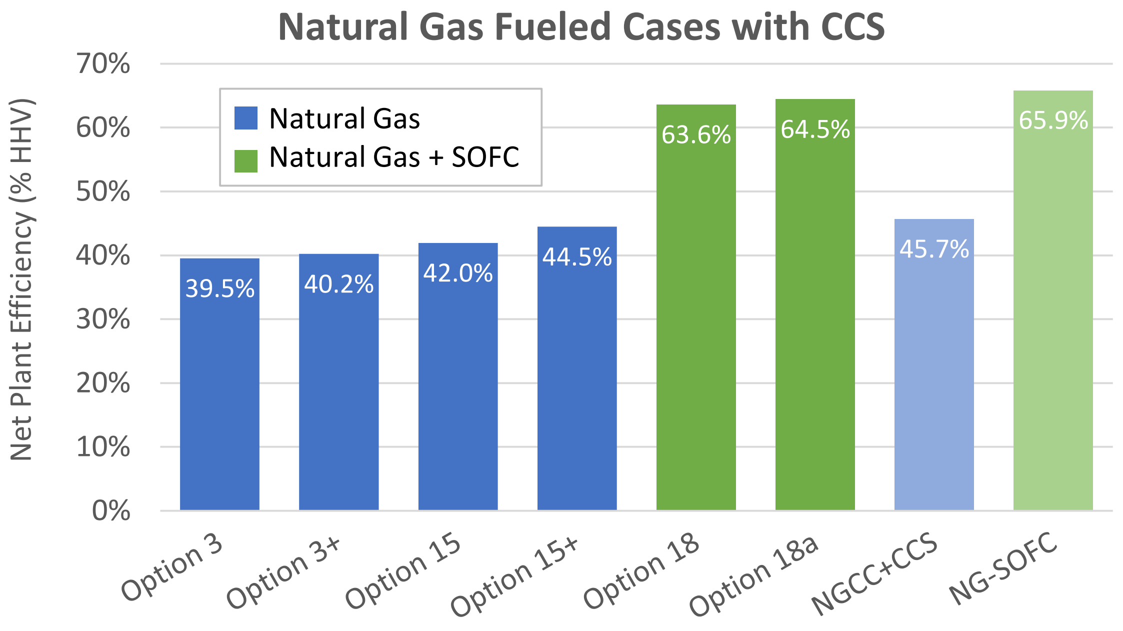

- **Option 2 (CO_2 Recycle) and Option 5 (Top Gasification) both outperform the baseline oxy-combustion system (Option 0)**
- **All MHD systems have higher efficiency than reference non-MHD cases**
- **Potential for further improvement with higher channel current density ("+" Options)**

- **Option 3 (open cycle MHD) and Option 15 (closed cycle MHD) are less efficient than the baseline NGCC system with CCS**
- **An advanced closed cycle MHD system (Option 15+) competitive with NGCC+CCS**
- **SOFC systems have much higher efficiency, but no improvement from MHD**

Combustion & Ionization Model

Predictive Model

- Electrical conductivity sub-model developed using existing approaches and updated MTCS data (Q_i) (Itikawa, Spencer, Collins)
- Subject of 2017 C&F paper[1]
- Lack of relevant experimental data necessitates direct validation (conductivity, electron #, temp)
- Sub-model has been integrated in OpenFOAM combustion model
  - Uses rhoreactingBuoyantFoam
  - Includes air entrainment in
  - Seed input modeled as gas phase

$$\frac{1}{\sigma} = \frac{1}{\sigma_{en}} + \frac{1}{\sigma_{ei}}$$

$$\sigma_{en} = \frac{e^2 n_e}{m\left[\frac{8kT}{\pi m}\right]^{1/2} \sum_{i=1}^{N} n_i Q_i}$$

$$\sigma_{ei} = 1.975 \frac{n_e e^2}{\overline{v_{ei}}}$$

Model considers both electron-neutral and electron-ion contributions

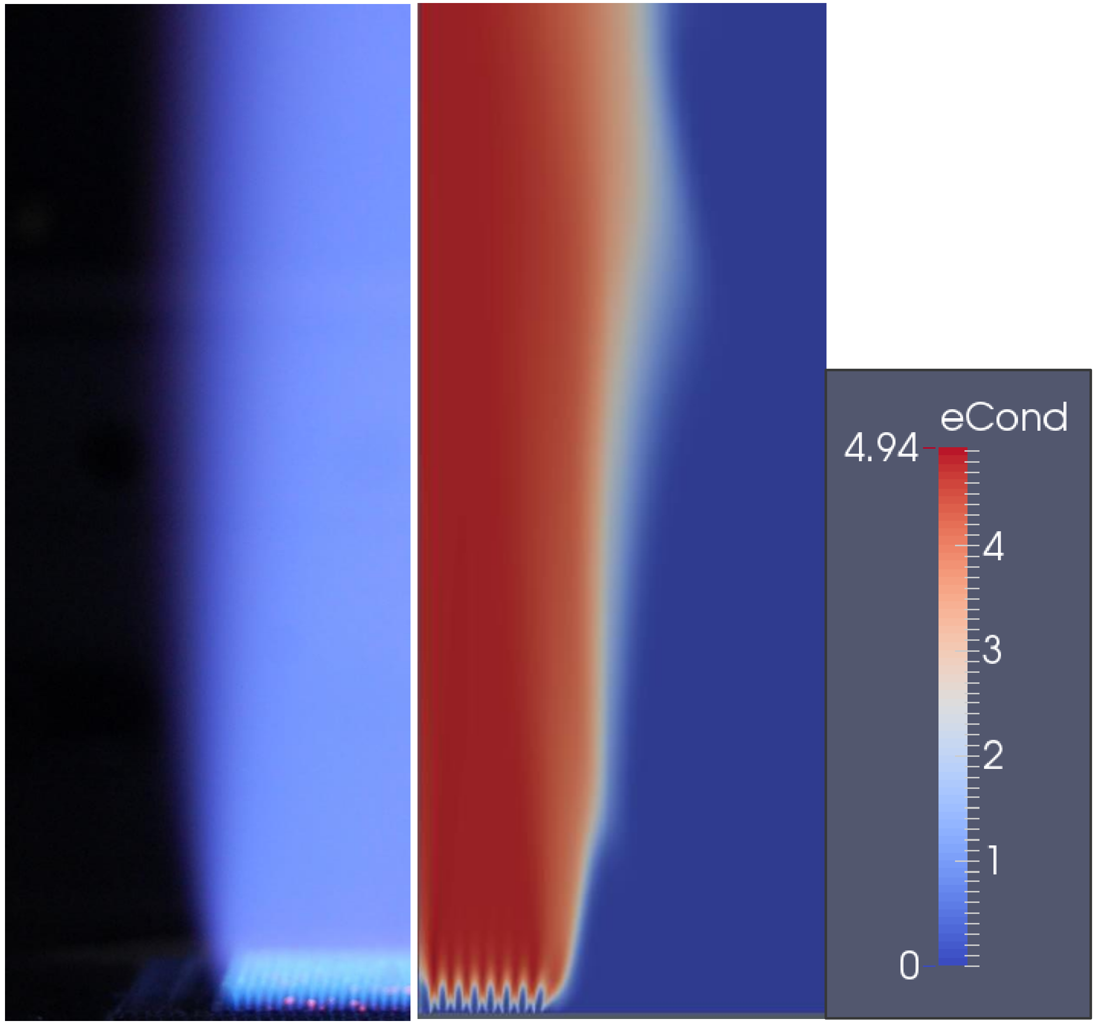

Image of Flame Model of Flame

[1]Bedick, C.R., Kolczynski, L., Woodside, C.R., "Combustion plasma electrical conductivity model development for oxy-fuel MHD applications", Combustion and Flame 181 (2017) 225–238.

Combustion and Ionization

Experimental Method & Results

Experimental Configuration

- Oxy-fuel Hencken burner
- Custom K_2CO_3 seed delivery system
- Provides wide range of combustion plasma conditions relevant to DPE

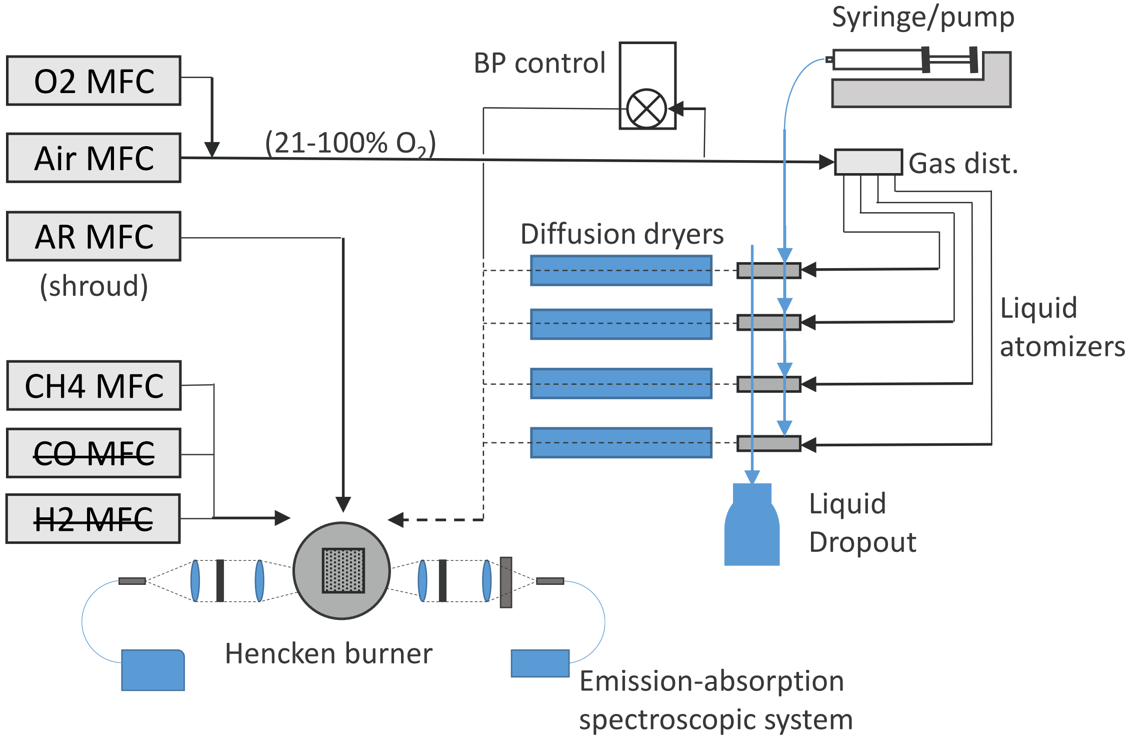

Emission-absorption spectroscopy:

- K atom #'s to verify seed delivery, construct profiles
- Gas temperatures
- Must consider effects of path-integrated measurement, K-band props for air-combustion

Langmuir probe (SLP, DLP):

- K^+ ion (~e^-), e^- temp
- Quantitative values from IV trace using appropriate probe model
- Rapid probe insertion to avoid tip melting
- Fresh Pt tips produce expected results
- Cooling from cold probe can affect e^- temp/conductivity

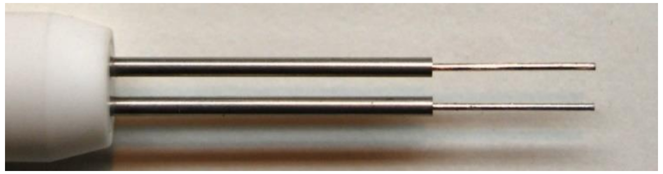

Langmuir double probe

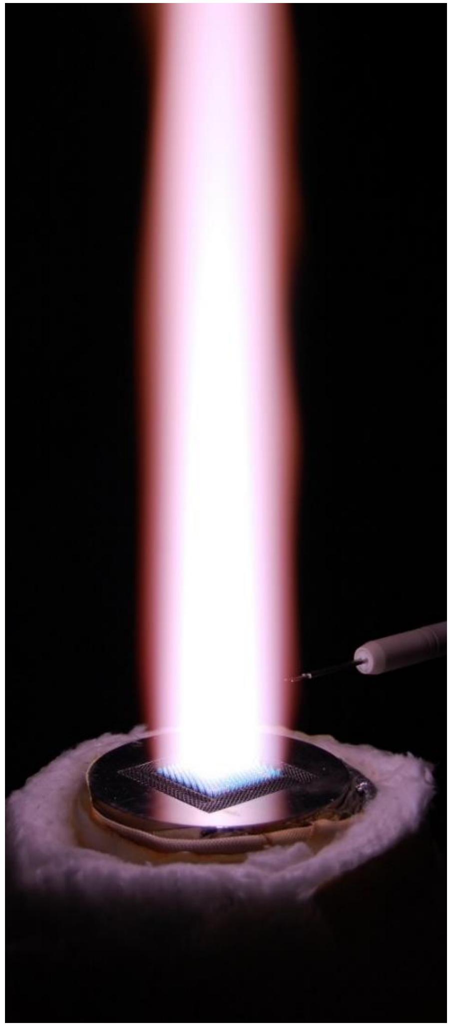

Combustion and Ionization

Experimental Method & Results

- Spectroscopic results for 100% O2, ~0.01% K compare well with OpenFOAM model
- Ion/electron results match equilibrium predictions at 25 mm (n_i ~2-3 x 10^{19} #/m^3, T_e ~3000 K)
  - Probe model (thin sheath-convection) fit to SLP saturation region to determine ion #'s
  - DLP slope through 0V dictates electron temp, conductivity

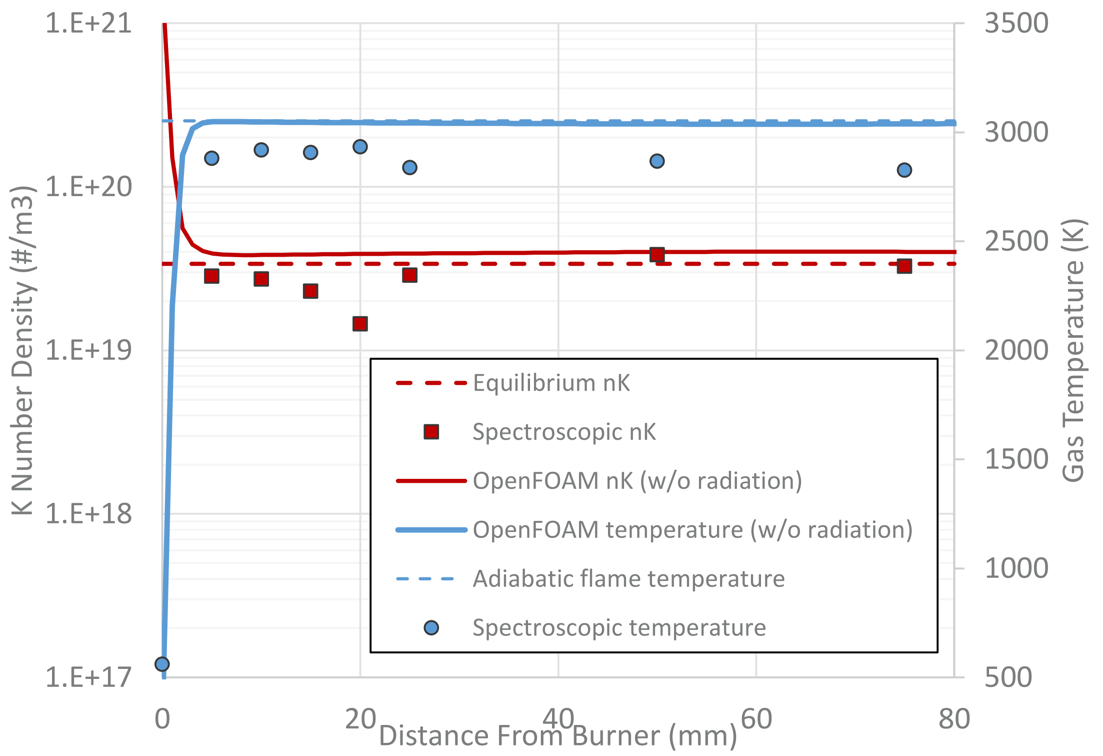

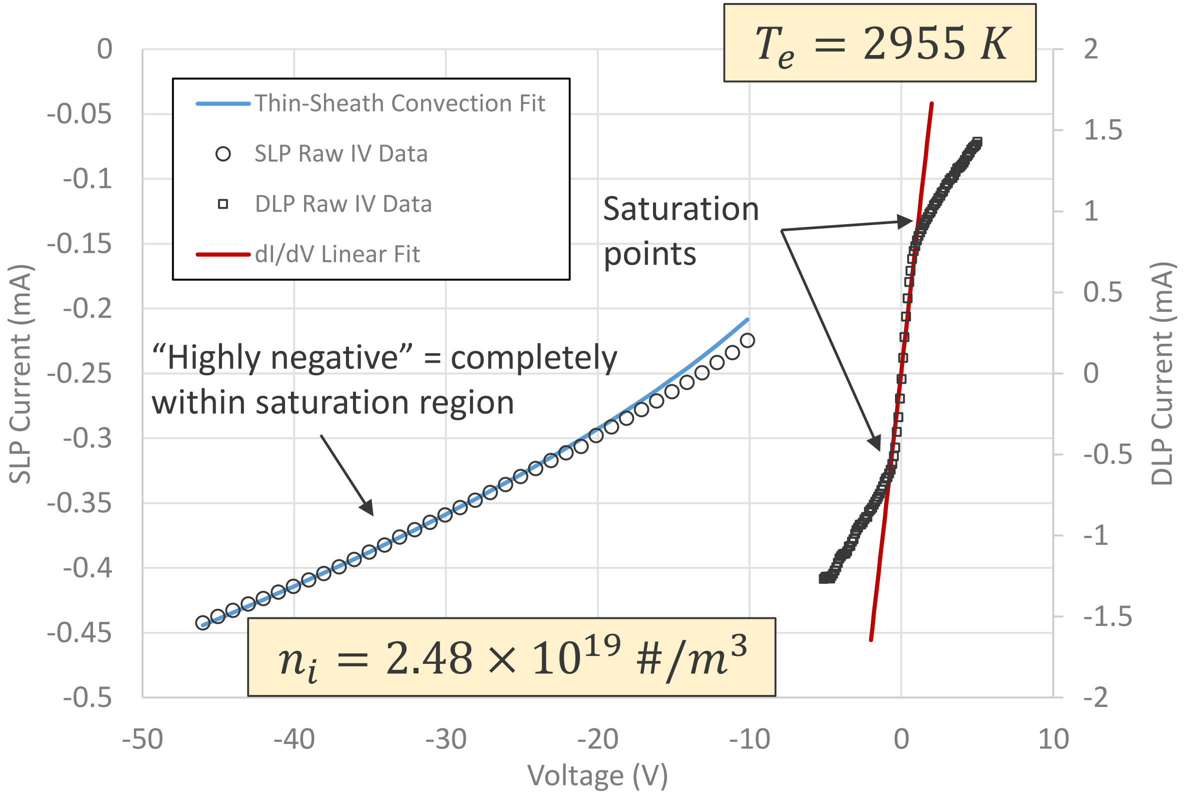

High Velocity Oxy-Fuel (HVOF) System

Multi phase combustion modeling with HVOF – Set-up & Simulation Set-up

- Customized Praxair JP 8200 HVOF utilized
- Kerosene-Oxygen Combustion
- 6-8 bar combustion
- ~160 kW_t Input Power
- Cold copper wall heat transfer
  - Use calorimetric method from cooling water temperature and mass flow measurements

<u>Simulation setup</u>

- Customized OpenFOAM model (userSprayFoam)
- 11 species with 10 reactions for combustion of Kerosene with surrogate dodecane ($C_{12}H_{26}$) from Choi2011AIAA
- PaSR (partially stirred reactor) combustion model
- 2D-axisymmetric and 3D-45degree domains

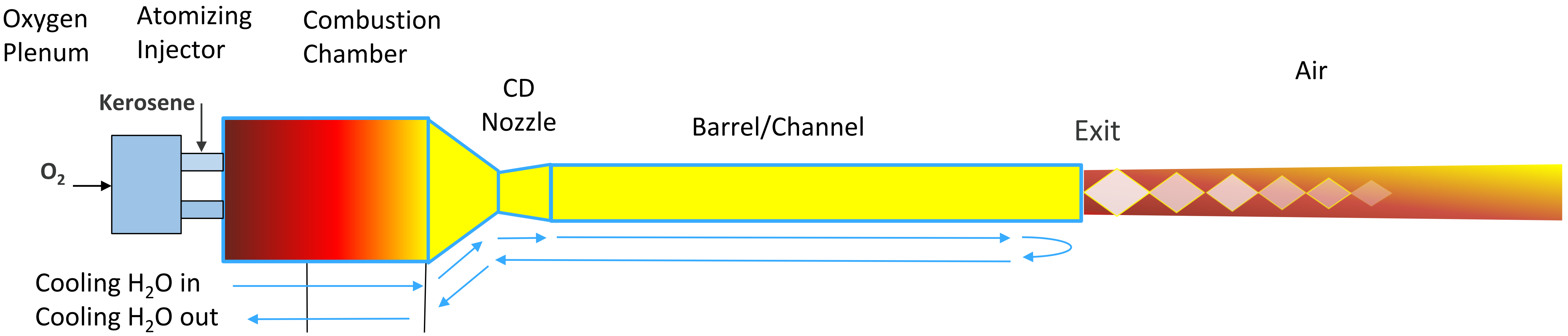

Establish a baseline cold wall heat transfer rate for future supersonic oxy fired MHD channels

High Velocity Oxy-Fuel (HVOF) System

Multi phase combustion modeling with HVOF –Simulation Results

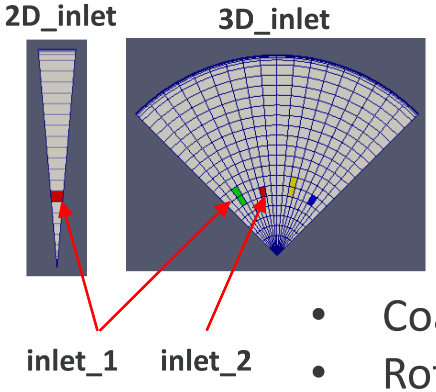

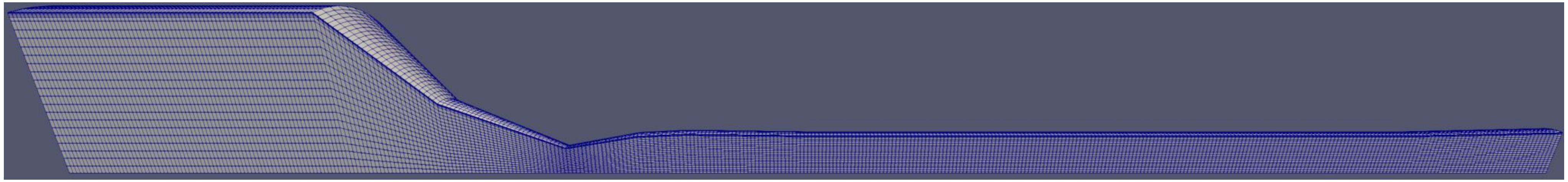

- Coarse Mesh Simulations
- Rotate the 2D mesh (10K cells) and generate the 3D mesh (180K cells)
- Mesh refinement (ratio = 0.5, 5 layers addition) at the boundary wall due to large gradient of T near wall

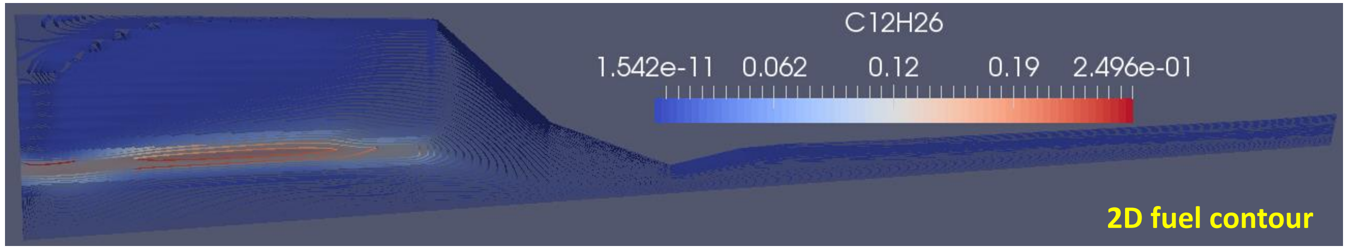

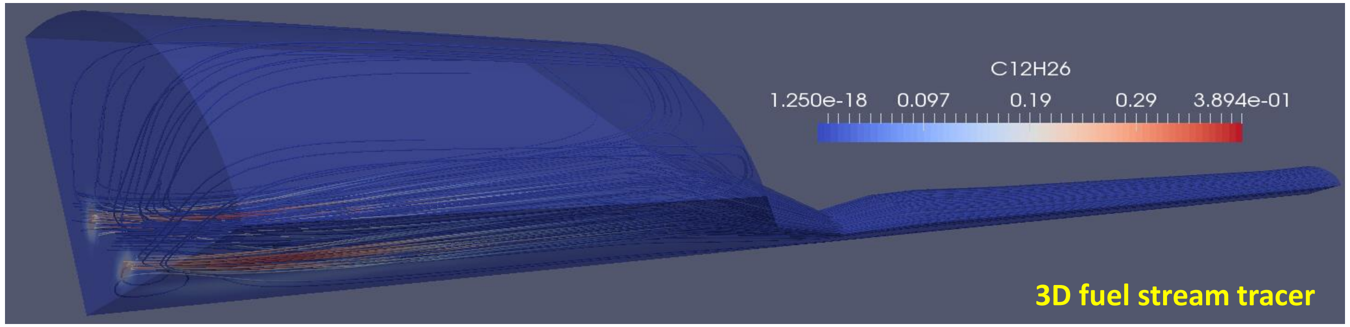

	Fuel	Oxygen
2D Gas fuel	inlet_1	inlet_1
2D Liquid fuel	injector	inlet_1
3D Gas fuel	100% Inlet_2	75% inlet_1 25% inlet_2
3D Liquid fuel	Injector	75% inlet_1 25% inlet_2

HVOF Total Wall Heat Transfer

Experiment versus simulation

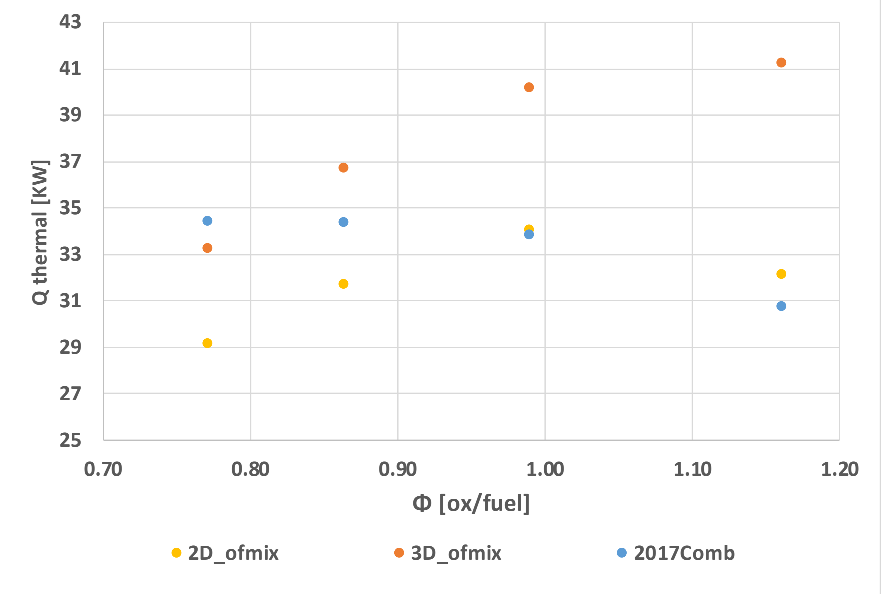

kW	2D Gas fuel (ϕ = 1.16)	3D Gas fuel (ϕ = 1.16)
Reaction Heat	119.82	126.06
Outer Wall	-32.10	-41.29
Inner Wall	-0.62	-2.21

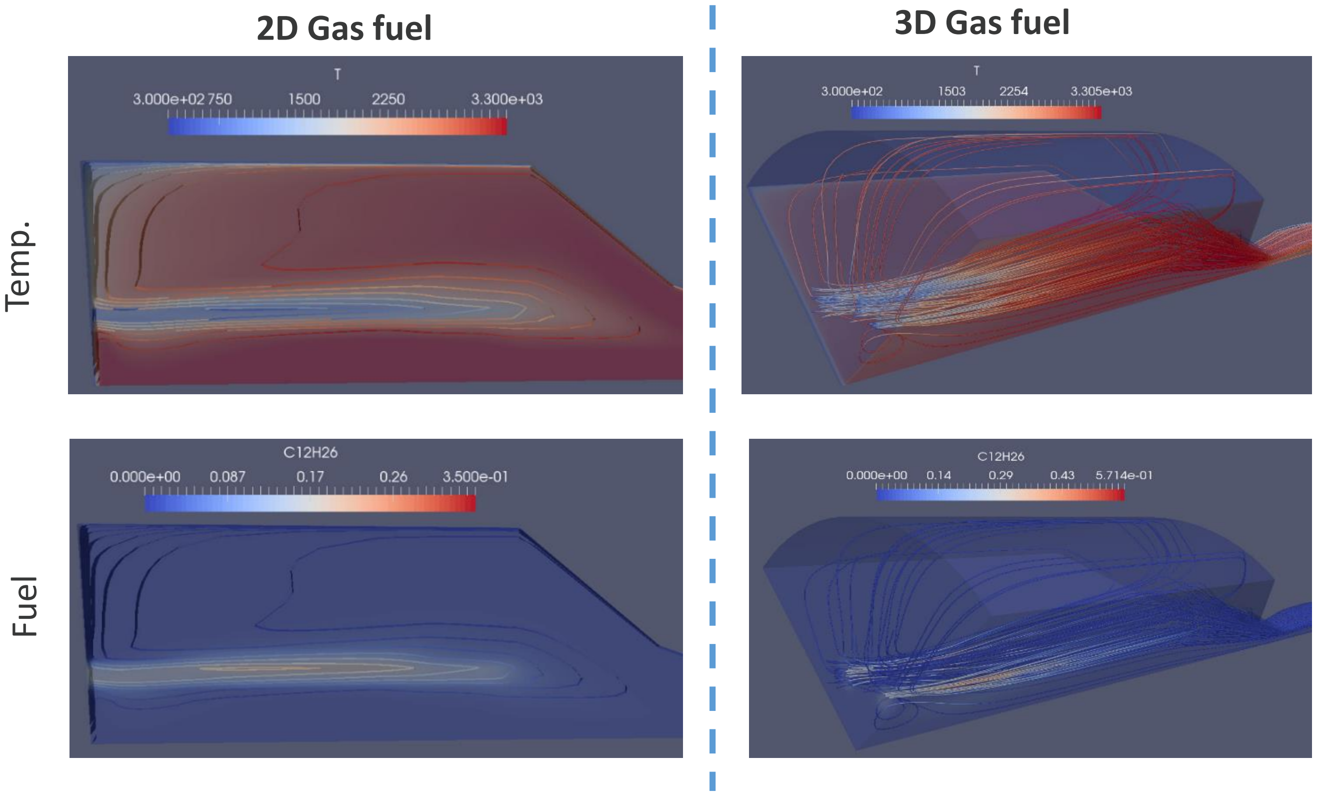

- 3D cases release more energy and leads to greater wall heat transfer – likely due to flame morphology and combustion chamber residence time (next slide)
- Currently investigating the effect of the liquid fuel droplet properties (droplet size distribution, injection speed, injection nozzle shape) on combustion efficiency

Wall heat transfer through wall for φ=1.16

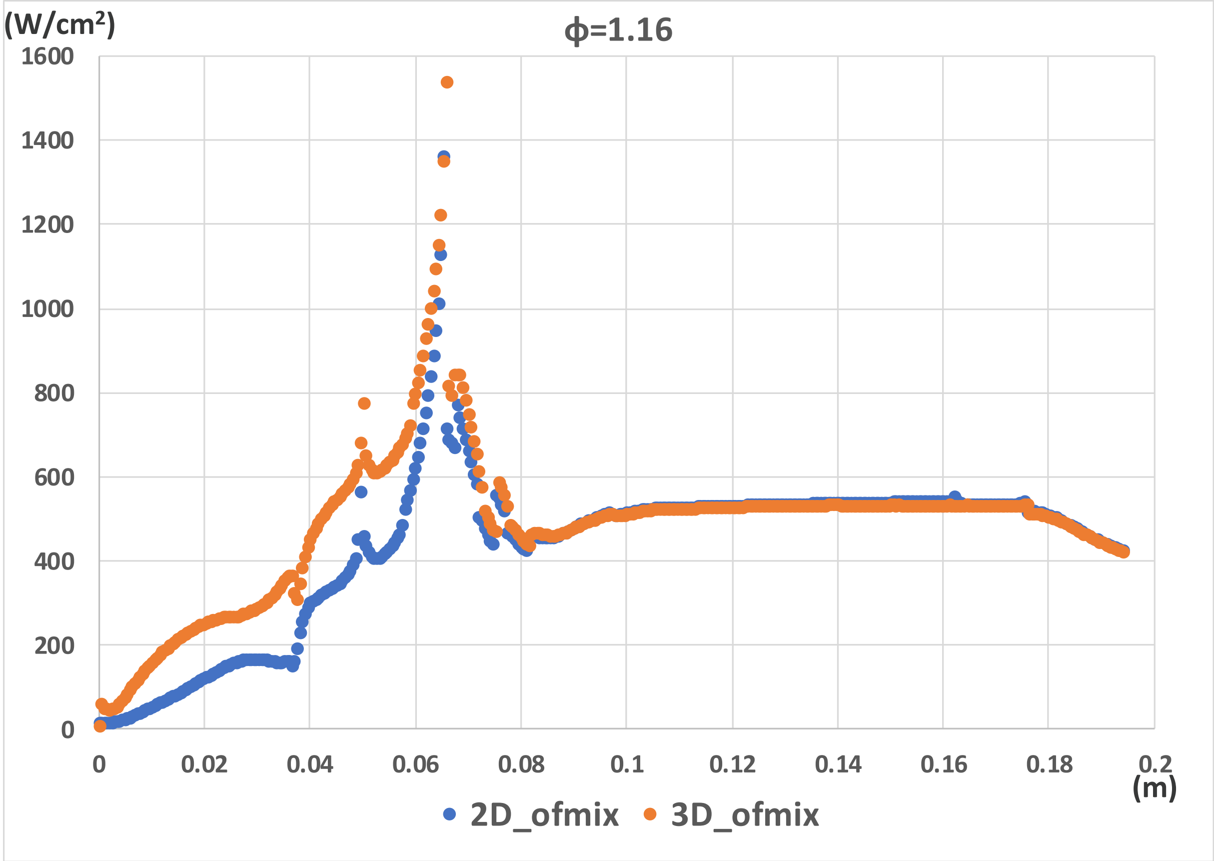

- Comparison of 2D_ofmix and 3D_ofmix of case $\varphi = 1.16$
- The higher heat transfer is shown at combustor for 3D case while it is consistent at barrel
- The higher combustion efficiency due to concentrated mixture and physical flame shape produces more higher heat transfer at combustor wall
- The distribution of oxygen into inlet_1 : inlet_2 (currently, = 3:1) and fuel droplet size distribution will change the combustion efficiency
- **In future also add: soot production and oxidation with radiation, mesh refinement**

CeO_2-base electrode materials

Electrical characterization

- CeO_2-Y_2O_3 and CeO_2-Gd_2O_3 based ceramics evaluated
- Impedance spectroscopy showed compositions rich in CeO_2 shows good conductivity values ~10 S/m for T>1500 K
- At low temperatures, electronic conductivity dominated and transitioned into an ionic conduction mechanism above ~900 K due to oxygen non-stoichiometry

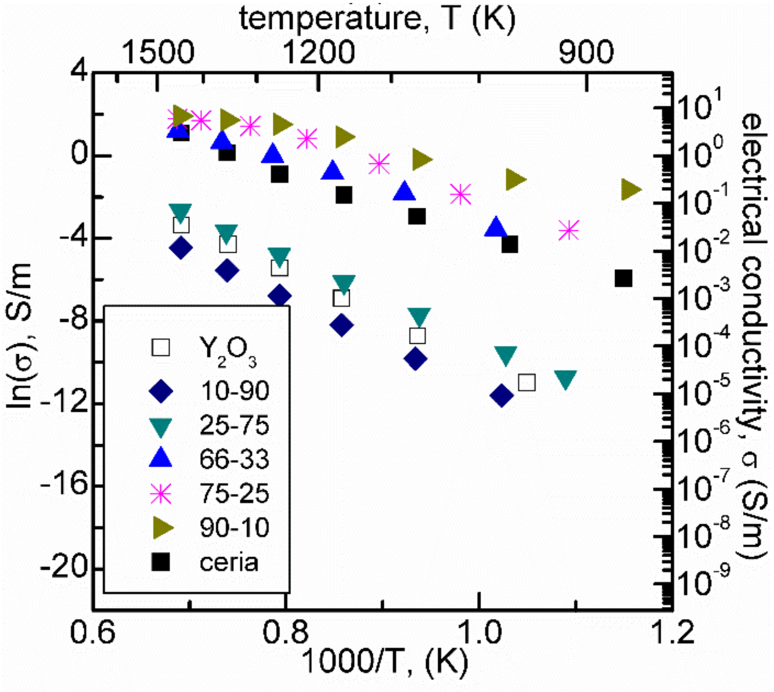

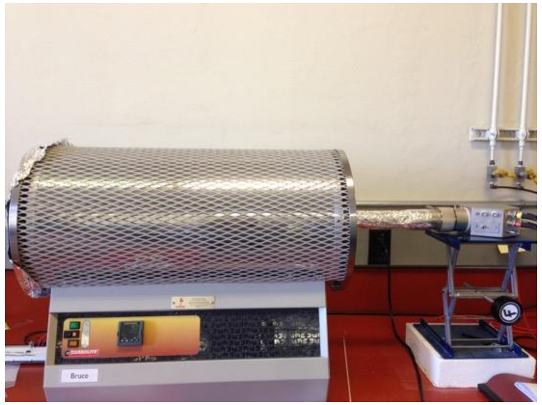

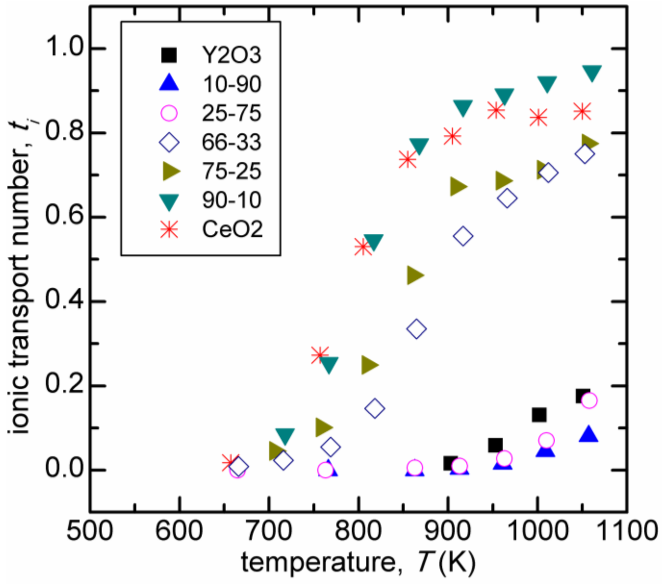

CeO_2-based electrode materials

Potassium Reaction Testing

- Oxide powders were mixed with K_2CO_3, pressed into green bodies and then fired at 1773 K for 1 hour
- After annealing in a K_2CO_3 environment, CeO_2, Y_2O_3, and Gd_2O_3 did not show any signs of reaction with K_2CO_3
- Overall, tests suggest that ceria-based ceramic electrodes show promise for use as electrodes in MHD power systems
  - Next step: HVOF exposure testing

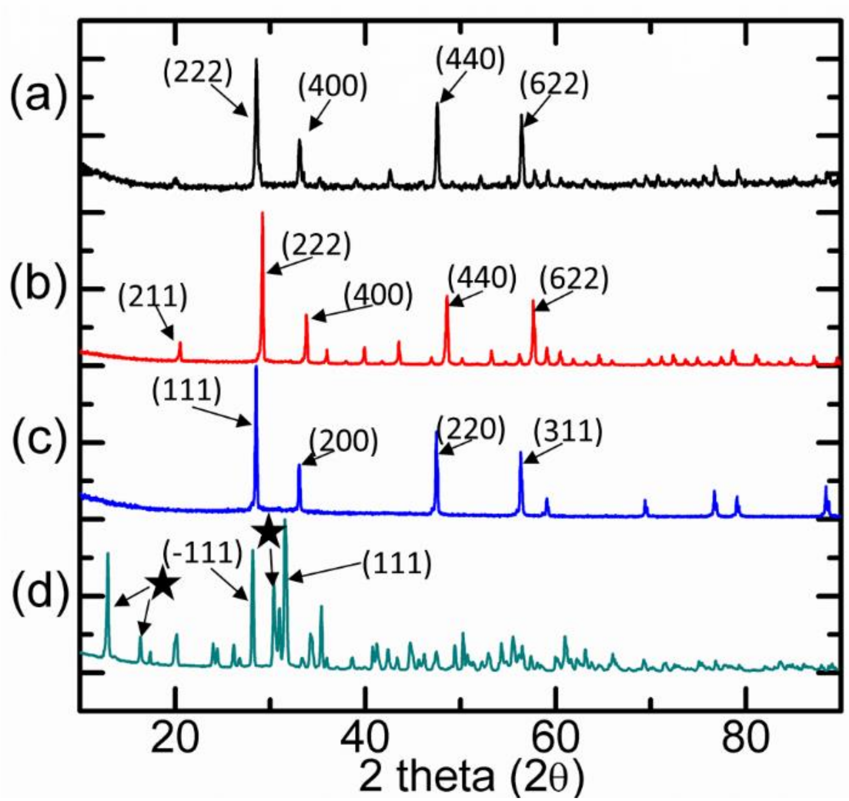

XRD patterns taken from (a) Gd_2O_3 (b) Y_2O_3 (c) CeO_2 and (d) ZrO_2. Peaks marked with a ★ can likely be attributed to the formation of $K_2Zr_2O_5$.

Electrode Material Testing

HVOF exposure testing

- **A new holder has been designed and built to test disc coupons of electrodes**
  - Nominal disc size: 1 cm dia. x 0.3 cm thick
  - Adjustable spring loading of disc to a MgO lip
  - Hot zone made of custom caste low density MgO
- **Test conditions under "free jet"**
  - Gas velocities est. 1000-2000 m/s
  - T_{static} gasses est. 2750 Kelvin
  - Pressures est. 1atm
- **Measured electrode materials data can be used as input to finite element modeling (FEM)**
  - Spacers (dwg #10,11,12) selected with desired thermal conductivity to reach some target temperature
  - Maximum sample temperature will be depend on sample thermal conductivity
- **Holder can be positioned by micrometers toward jet edge**
  - T gradients at jet edge ~300K/mm according to CFD modeling
  - Hot side surface temperatures monitored by custom 2-color pyrometer

New holder

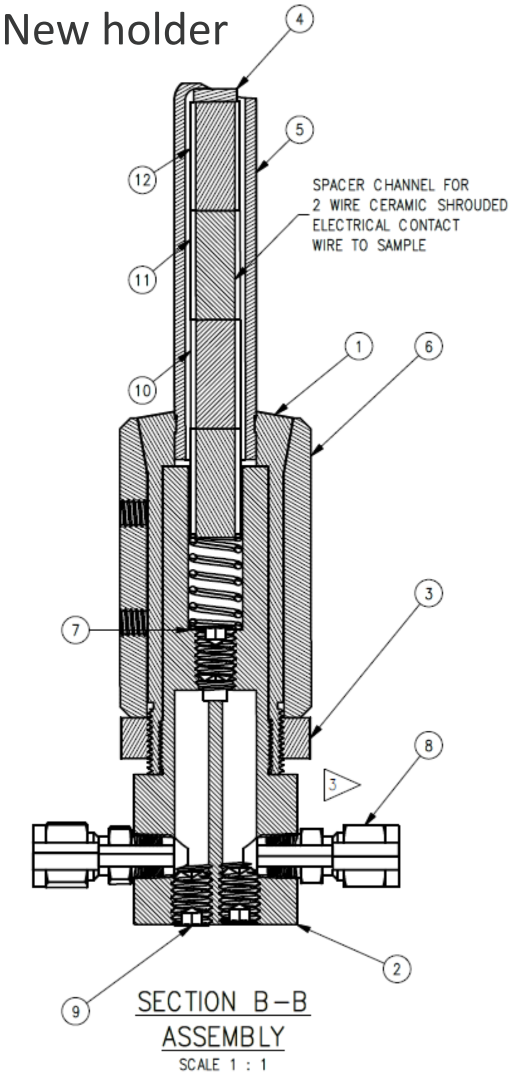

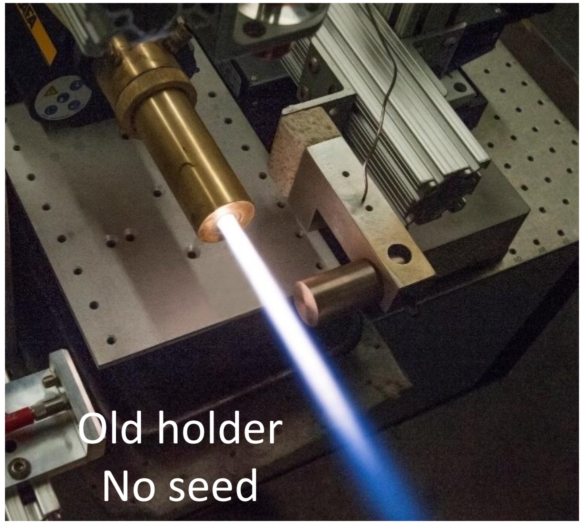

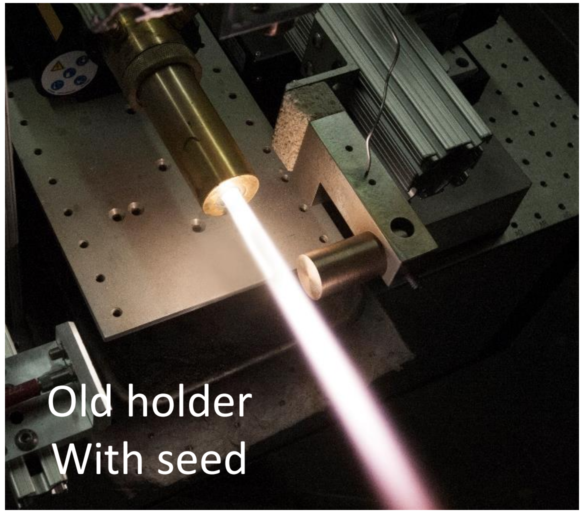

FEM of new holder

NATIONAL ENERGY TECHNOLOGY LABORATORY

Showing expected exposure temperatures and heat fluxes

q_0=h∗(T_ext−T)
Convection eq

T_ext = 2750K

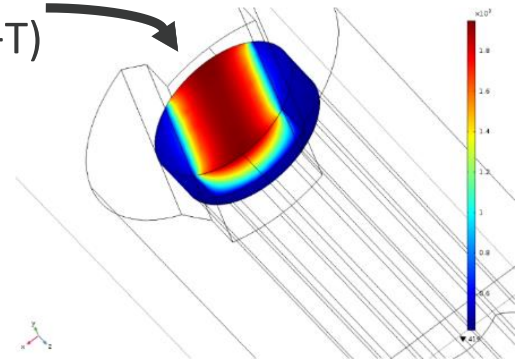

If the sample k = 1 W/mK

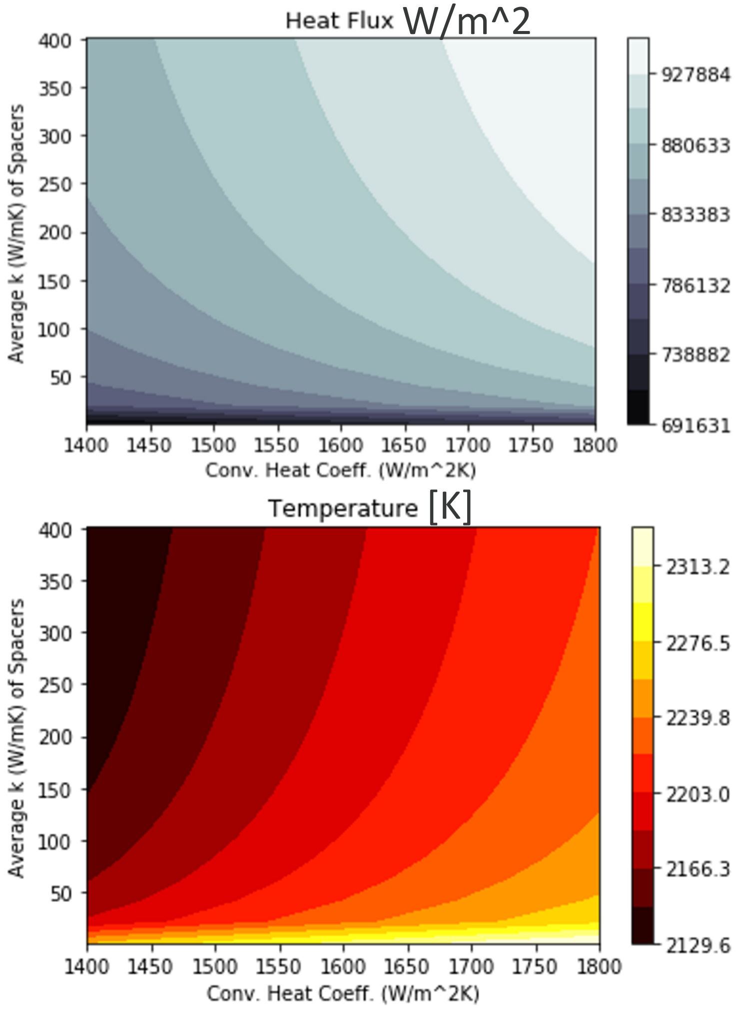

If the sample k = 10 W/mK

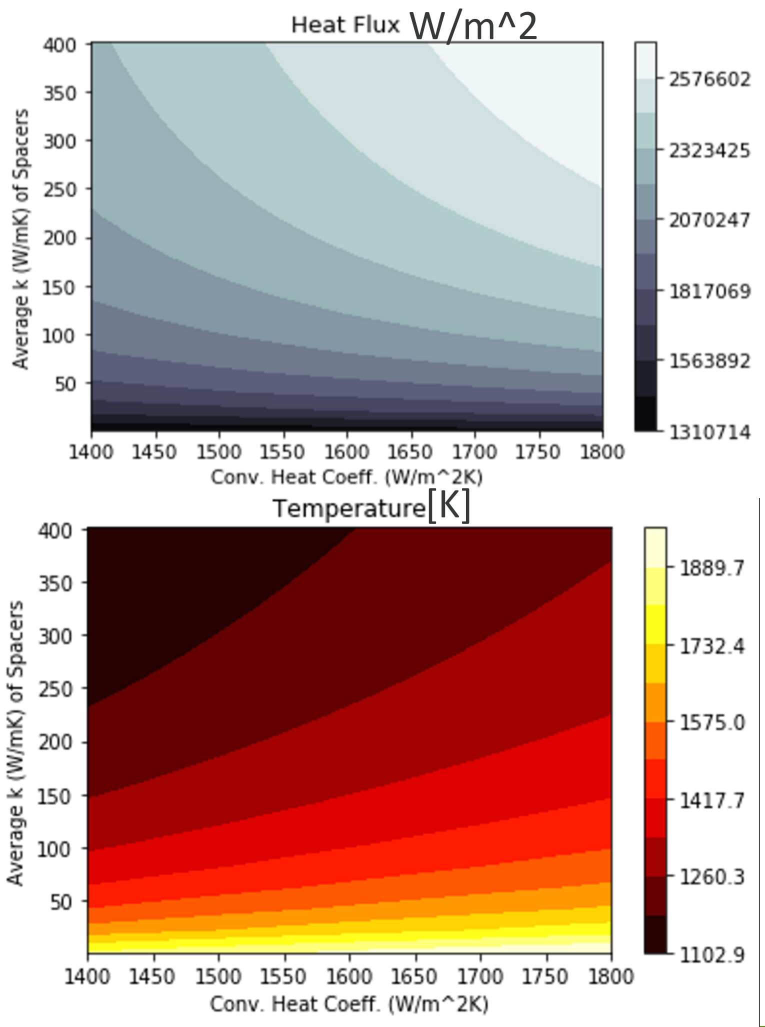

- **Maximum sample temperatures**
  - Spacer conductivity
    - Provides more control with higher k sample
  - For k = 1 sample (e.g, ceria)
    - Should hit target service temp >1800 C
  - For k = 10 sample
    - In service max temps ~1100 to 1900K.
  - Continued model refinements underway
  - Validation testing now started

Photoionization Enhancement

Creating a non-equilibrium plasma using photons.

- **Combustion driven MHD plasma is a partially ionized system which rapidly reaches thermal equilibrium**
  - Very little seed introduced thermally ionizes (~1-3% of it)
- **Ionization potential of K is 4.34 eV**
  - "photoionization" of K using UV photons < 285nm
  - UV source must be efficient enough to make sense for bulk ionization > 10% efficiency past gross estimate (Rosa, 1963)
- **Directed energy with lasers = Good spatial & temporal control**
  - Boundary layer arc control and manipulation possible
    - "Help" electrons travel from plasma to cooler electrode to reduce loss mechanism of voltage drop
    - Voltage drop must be overcome to make this work at small scale
  - Note that due to arcs the boundary layer is already likely in thermal non-equilibrium

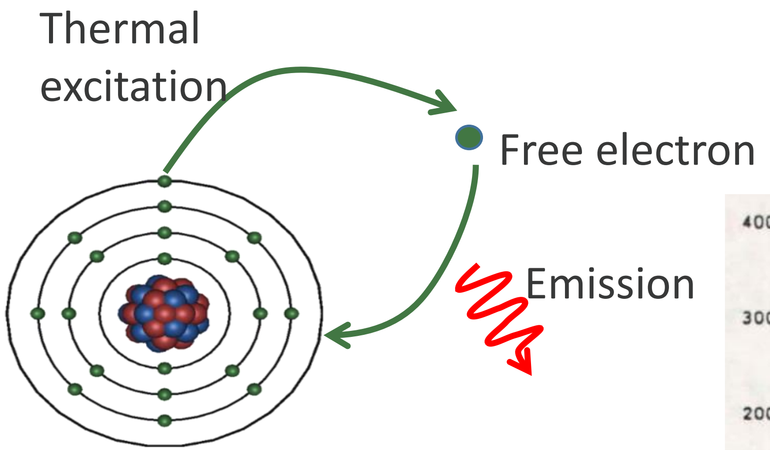

Potassium

With thermal Ionization of K

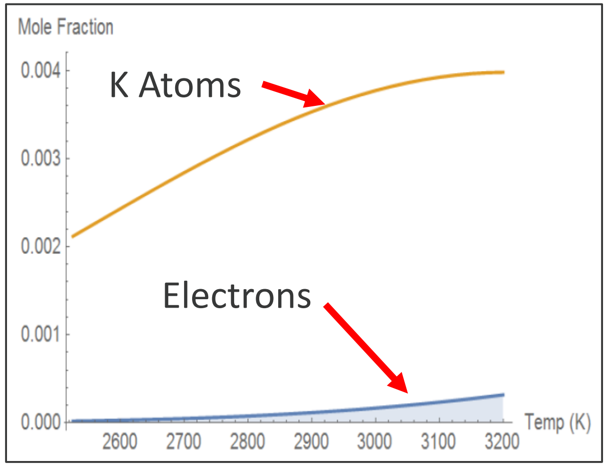

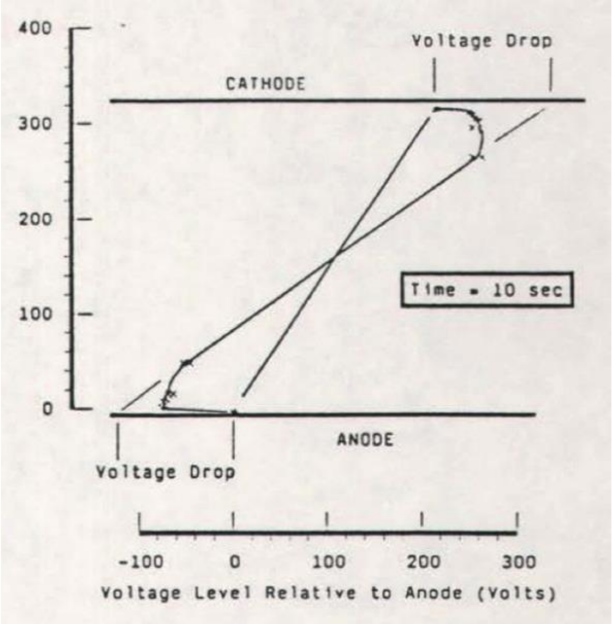

0.32m x 0.145m Segmented Faraday Generator. Sub-sonic oxy-fuel, hot ceramic electrodes ~32.5MWt

Voltage drop plot from UTSI-IEE Testing reported by Lineberry, 1988.

CFD Model with photoionization

Enhancing a partially ionized seeded oxy-combustion plasma in thermal equilibrium

- **OpenFOAM CFD model of photoionization**
  - Customized solver based on reactingParcelFoam and sonicFoam
- **Fluid –** conservation of mass, species, momentum and energy
  - $\frac{\partial \rho}{\partial t} + \nabla \cdot (\rho \boldsymbol{u}) = S_p^{\rho}$
  - $\frac{\partial \rho_i}{\partial t} + \nabla \cdot (\rho_i \boldsymbol{u} + \rho_i \boldsymbol{v_i}) = \kappa R_i + S_p^i$
  - $\frac{\partial \rho \boldsymbol{u}}{\partial t} + \nabla \cdot (\rho u u) = -\nabla p + \nabla \cdot (\boldsymbol{\tau}) + S_p^u$
  - $\frac{\partial \rho E}{\partial t} + \nabla \cdot (\rho \boldsymbol{u} E) = -\nabla \cdot \boldsymbol{q} - \nabla \cdot (\boldsymbol{u} p) + \nabla \cdot (\boldsymbol{u} \cdot \boldsymbol{\tau}) + S_p^h$
- **Turbulence -** k-ω SST turbulence model with a high-Mach number compressibility correction
  - $\frac{\partial \rho k}{\partial t} + \nabla \cdot (\rho u k) = \nabla \cdot \left(\left(\mu + \frac{\mu_t}{\sigma_k} \right) \nabla k \right) + S_k$
  - $\frac{\partial \omega}{\partial t} + \nabla \cdot (\rho u \omega) = \nabla \cdot \left(\left(\mu + \frac{\mu_t}{\sigma_k} \right) \nabla \omega \right) + \left(\beta - \frac{K^2}{\sigma_\omega \sqrt{C_\mu}} \right) \frac{\omega}{k} P_k - \beta \omega^2$

Reaction Model	
Methane Oxidation Modified Jones-Lindstedt	$CH_4 + 0.5\ O_2 \rightarrow 2\ H_2 + CO$ $H_2O + CH_4 \rightarrow 3\ H_2 + CO$ $H_2O + CO \leftrightarrow H_2 + CO_2$ $H_2 + 0.5\ O_2 \leftrightarrow H_2O$ $O_2 \leftrightarrow 2\ O$ $H_2O \leftrightarrow H + OH$
Potassium Ionization	$K^+ + e + M \leftrightarrow K + M$ $OH + e + M \leftrightarrow OH- + M$
Photoionization	$K + hv(248nm) \rightarrow K^+ + e$

Photo-ionization reaction using the Arrhenius equation
- $P = cQ_{ph}\, n_\lambda\, [K]$
- $P = k_f n_\lambda [K] = AT^b e^{(-E_a/RT)} n_\lambda [K]$
- Q_{ph} =3.37×10^{-24} m^2 from literature

  -> $cQ_{ph} = AT^b e^{(-E_a/RT)}$

  -> A = 1.01×10^{-15} m^3/s, b = 0, E_a = 0

Laser and thermal radiation sub-model

Radiative Transfer using discrete transfer method (DTM) and P1-method

- **Collimated radiation from the laser and thermal radiative**
  - $I(\hat{s},\lambda) = I_c(\hat{s},\lambda) + I_D(\hat{s},\lambda)$
- **Collimated radiation using Beers Law**
  - $\frac{dI_c}{ds} + (\kappa+\sigma)I_c = 0 \quad \rightarrow \quad I_c(s) = I_c(s=0)e^{(-(\kappa+\sigma)s)}$
- **Diffuse radiation using a P1-method including interaction with collimated radiation**
  - $\hat{s}\cdot\nabla I_D + (\kappa+\sigma)I_D = \kappa I_B + \eta + \frac{\sigma}{4\pi}\int I_D(\hat{s_i})\Phi(\hat{s_i},\hat{s})d\Omega + \frac{\sigma}{4\pi}\Phi(\hat{s_i},\hat{s})I_c$
- **Absorption coefficient using the partial Planck mean coefficients from RADCAL**
  - $\kappa = Q_{ph}N_A[K]$

Model and Experiment Set-up

For Testing Photoionization

- Free jet shock structures impact local T and species
- Multiple laser passes used to increase response and overcome flow non-uniformities
- Heat Loss results checked against HVOF heat balance data reported in 2017
- Our main interest is ion-electron recombination time following laser pulse

Table 2. Geometry and boundary conditions of combustor and exhaust simulations

System geometry	Combustor diameter, length (cm)	1.91, 3.70
	Nozzle throat diameter, length (cm)	0.64, 4.45
	Nominal barrel diameter, length (cm)	1.0, 11.31
	Mesh size (cm)	~ 0.04
Combustor Inlet	Equivalence Ratio	~ 3.5
	Oxygen/Fuel Ratio	~ 4.0
	Potassium ratio, wt%	1.25, 2.5, 5
Wall	Temperature, K	340
	emissivity	1

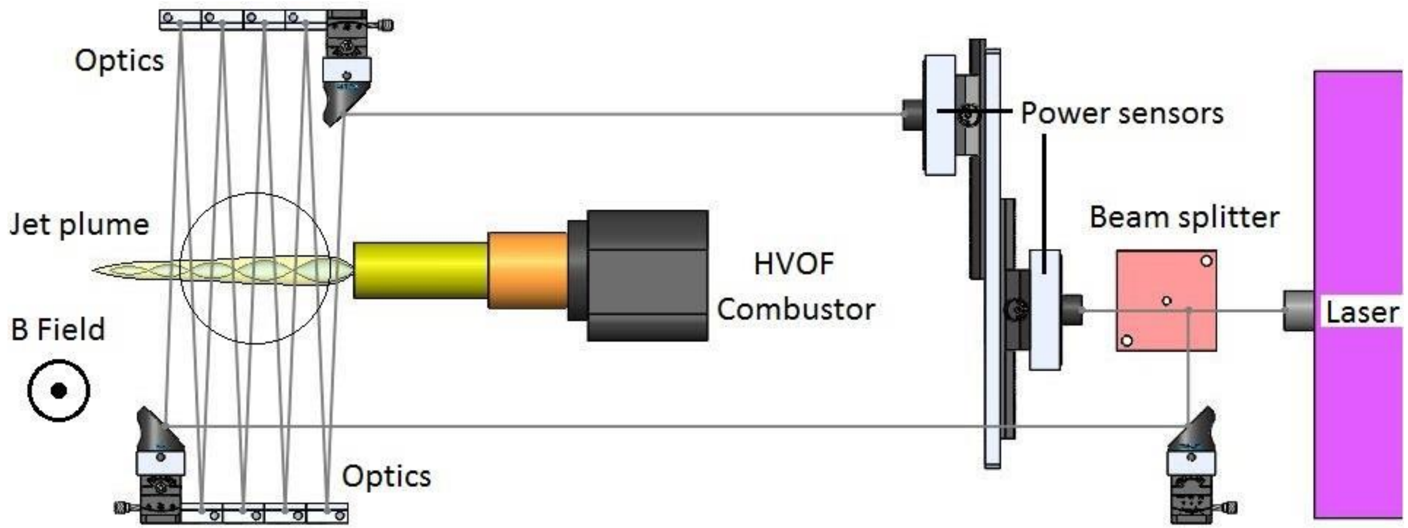

Table 4. Laser and photoionization parameters

Pulse duration	9 ns
Power per pulse	20 mJ
Peak power during pulse	2.2MW
Photons per pulse	$2.5\text{x}10^{16}$
Beam dimensions Vertical x Horizontal	2mm × 6mm
Peak intensity	0.18×10^{12} W/m^2
Pulse frequency	< 100 Hz
Vertical distance between mirrors	31 cm
Horizontal distance between mirrors	31 cm
Laser Incidence Angle	~2.3°
Pre-exponential Factor for Photoionization Reaction $K + \text{photon} = K^+ + e^-$	0.6084×10^{12} m^3/kmol/s

Photoionization HVOF Model & Experiment

Results

- **Time resolved spectroscopy with nanosecond level time resolution used in the experiment**
  - Measure emission for K excitation at ~767nm doublet as proxy for changes in free electrons
- **model and experiment show boost during laser pulse**
- **Model shows persisting non-equilibrium plasma following laser pulse, experiment does not.**

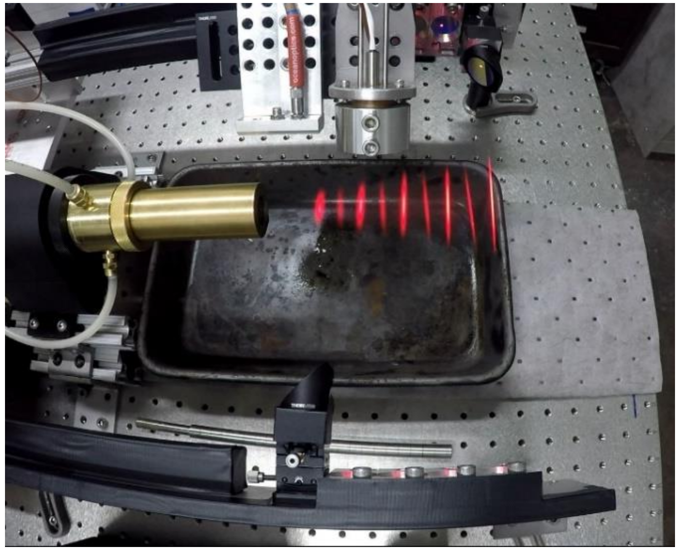

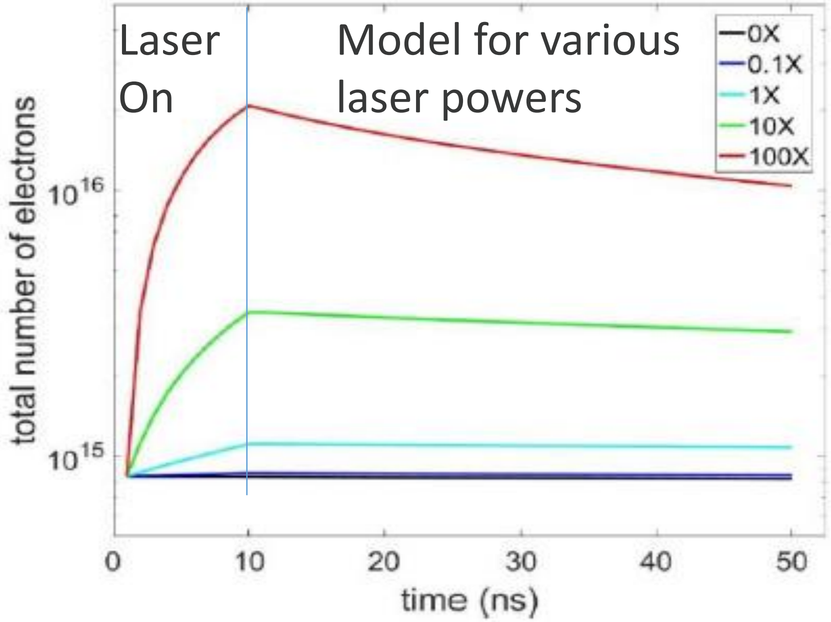

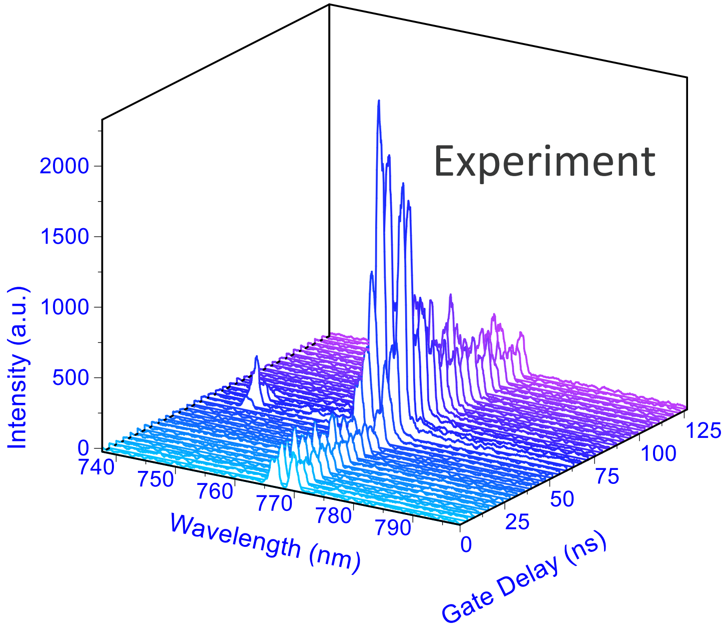

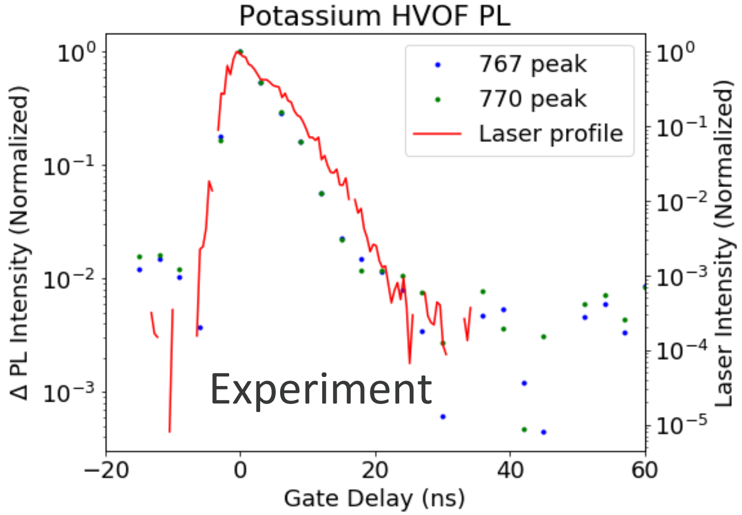

Photoionization Alkali Vapor Experiment

Investigating why HVOF model and experiment recomb time differed.

- Use quartz test cell containing Rb under high vacuum (will also test K, Na, and Cs)
- Test at ~330K, Expect p ~ 8*10^-6 Torr
- Photo-ionization achieved
- Recomb time lasts ~6 microseconds following laser

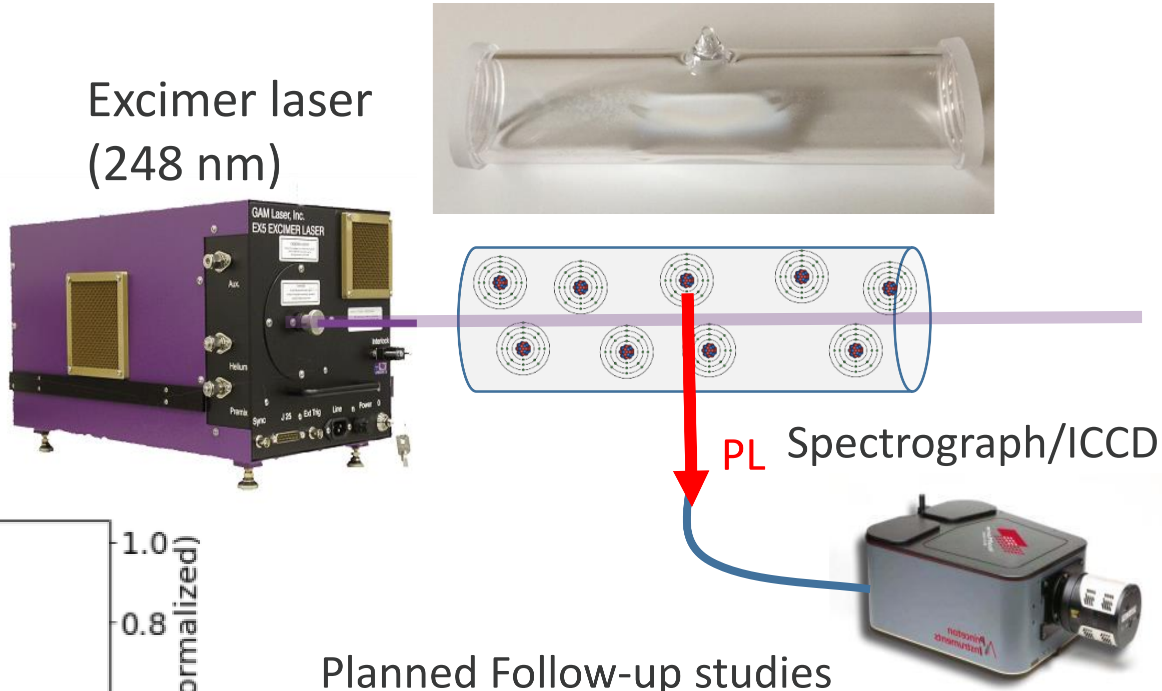

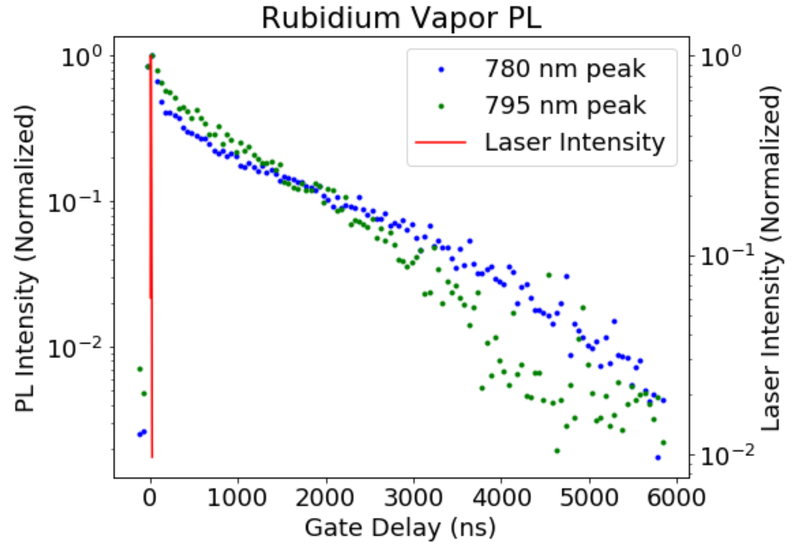

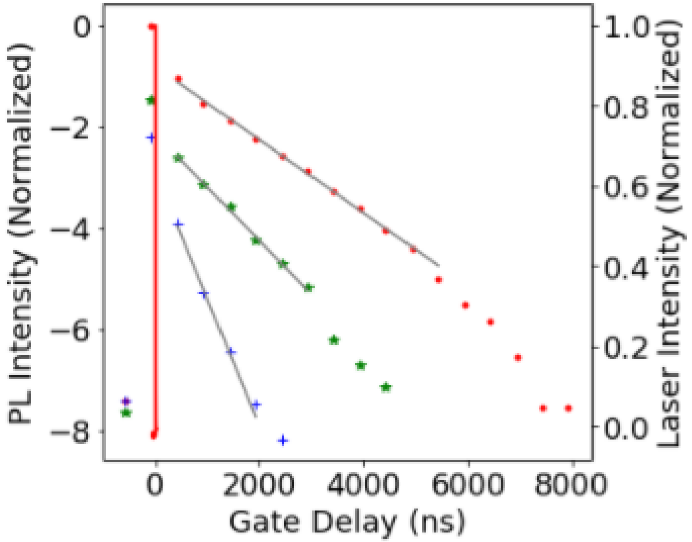

Planned Follow-up studies

- Model this system
- Investigate non-linear effects
  - Surface ejection of alkali?
- Other alkalis
- Sensitivity to laser power and cell temperature

Conclusion

This project expected to continue for another 2 years before a go/no-go decision

- **Coal power systems with DPE have similar efficiencies and can offset O_2/CCS efficiency cost**
  - MHD power density increases will improve efficiency further
  - Cost and difficulty for system may become determining factor for further development
- **Seeded Oxy-methane combustion conductivity measurements consistent with published model so far**
- **HVOF Wall heat transfer very sensitive to modeling parameters**
  - CFD uncertainty quantification needed to parameterize this term for performance evaluation
- **Electrode samples fabricated which do not react with potassium and show sufficient electrical conductivity (in static testing)**
- **HVOF materials test rig model shows wide range of service temperatures possible**
  - Though highly depend on the material's thermal conductivity
- **Model and experiment of non-equilibrium plasma generation in combustion products did not agree**
  - Further experimentation underway to understand this

Acknowledgment

Thanks to NETL/DOE FE's Cross Cutting Research Group for the support.